A Large-scale Structural Mixing Model applied to Blowout of Turbulent Nonpremixed Jet Flames in a Cross air-flow

KEE MAN LEE* (LG Electronics Inc.) and HYUN DONG SHIN (KAIST)

Keywords : cross flow, large-scale structural mixing model, counter-rotating vortices, local mixing time, characteristic chemical reaction time, liftable flame, blowout limit, blowout distance, blowout parameter

Abstract

This article presents an application of a large-scale structural mixing model (Broadwell et al. 1984) to the blowout of turbulent reacting jets discharging perpendicularly into an unconfined cross air-flow. In an analysis of a common stability curve, a plausible explanation can be made that the phenomenon of blowout is related only to the mixing time scale of the two flows. The most notable observation is that the blowout distance is traced at fixed positions at all times according to the velocity ratio R. Measurements of the lower blowout limits in the liftable flame agree qualitatively with the blowout parameter ε, proposed by Broadwell et al. Good agreement between the results calculated by a modified blowout parameter ε' and experimental results confirms the important effect of a large-scale structure in specifying the stabilization feature of blowouts.

1 Introduction

The jet in cross flow is an important problem from both a practical and a fundamental fluid dynamics point of view. The most obvious feature of the jet in the cross flow is the mutual deflection between the jet and the cross flow. These motions stress the importance of the existence of a large-scale vortical structure. A considerable number of studies have been conducted in an attempt to understand how these vortices structures might affect jet growth, mixing, and entrainment in this flow field.[1-5] The main role of such large-scale structures on flame structure has been explained by many investigators[6-9]. However, not much investigation has been done on flame stability, especially the phenomenon of lift-off and blowout.

The jet blowout literature can be roughly classified into two generally proposed phenomenological theories[10]. One of the theories is the premixed combustion model proposed by Vanquickenborne and Van Tiggelen[11] in the mid-1960s. This model describes that blowout occurs when the local flow velocity exceeds maximum premixed turbulent burning velocity. The second theory addresses the main role of large-scale structures[13-15]. In particular,

Broadwell et al.[13] suggested the large-scale structural mixing model, and postulated that blowout could be due to the quenching of reaction when the molecular mixing rate in the flow becomes sufficiently large. In this viewpoint, the existence of a large-scale vortical structure might be the key to understanding flame stability, including liftoff and blowout. A plausible explanation could be drawn to blowout mechanism by the large-scale structural mixing model. However, despite a few studies[13,14] on the application of this model in a stagnant ambient air and co-flowing air stream, the application of this model to a cross flow field has not yet been made. This motivates the present study.

The focus of the present investigation is mainly on the possibility of the application of the blowout model of Broadwell et al to blowout in a cross air-flow, ascertaining the importance of large-scale vortical structures on flame stabilization. In particular, we examine the lower blowout limits of a liftable flame.

2 Experimental set-up and measuring method

Figure 1 shows the schematic configuration of this experimental study and the adopted coordinate system. The experiments were carried out in an open jet wind tunnel of an 0.5 m by 0.7 m cross section for cross flow velocities ranging from 0 to 9 ms^{-1}. The fuel nozzle was protruded vertically 100 mm above the bottom of the test section so that it did not interact with the wall boundary layer. Fuel was supplied through circular nozzles of various diameters. The nozzles were stainless steel tubes with sizes ranging from 1.6 mm to 5.3 mm in inner diameter and a length of 100 d_o to assure a fully developed flow at the nozzle exit. A settling chamber was also installed to suppress flow disturbance. The mean cross flow velocity was carefully taken to ensure a low level of turbulence intensity in the wind tunnel flow by constructing a honeycomb and three layers of screens. The turbulence intensity at a cross flow velocity of 5 ms^{-1} by a hot wire anemometer was less than 1.0 %. During the experiment, the cross flow velocity was continuously monitored with a pitot tube.

The Reactive-Mie-Scattering (RMS) technique was employed to identify the existence of large structural vortices of nonreacting jets at locations corresponding to blowout distances. For the RMS technique, particles formed easily by a chemical reaction between the ambient moisture and gaseous $TiCl_4$. Thus, immediately after fuels were injected from the nozzle exit, $TiCl_4$ formed TiO_2 particles in the mixing layer between fuel jet and cross flow. Color photographs with a long time (about 1s) exposure were taken to determine the blowout distance and the kidney shaped width of a deflected jet. The blowout distance was defined as the curvilinear length from the nozzle exit to the central point of the flame base along the center line of the deflected jet[6], which was visualized by Mie scattering with the kerosene smoke particles.

3 Results and discussion

3.1 General features

1) Stability curve

There are two types of flames in the turbulent jet diffusion flame with the cross flow[16]. One is the liftable flame, which can persist to blowout once the flame is lifted. The other is the never-lift flame that blows out immediately when the flame lifts off from the jet nozzle, thus preventing the formation of a lifted flame. Kalghatgi[17] conducted experiments on blowout stability limits in the liftable flame. Huang et al.[16] examined flame stability in the never-lift flame. Figure 2 shows the stability domains of the liftable and never-lift flames obtained with various nozzle diameters. In the present study, the primary concern is the stabilization mechanism of the lower limits of liftable flame, which might be associated with the large-scale structural mixing model. Figure 3 shows that the stability limits obtained in this experiment are similar to those presented previously by Kalghatgi[17]. Although the author do not note it, careful observation in Fig. 3 reveals that blowout conditions are well expressed as time scales of the two flows, fuel jet and cross air-flow. This alludes implicitly that the phenomenon of blowout is strongly related to the mixing time scale of the two flows. Therefore, we apply the mixing time concept of the large-scale structural mixing model to the description of the blowout mechanism.

2) Flame shape near blowout at lower blowout limits

Figure 4 shows a typical still photographs of the flame base just prior to blowout. Here, it is known explicitly that the flame location shown in Fig. 4-a corresponds to blowout distance. It is notable that the flame shapes shown in Fig. 4-a always appear in the lower limits of the stability curves, regardless of nozzle diameter. The flame base, which is completely filled with blue flame, shows a typical kidney shape. Occasional streak-like soot particles also appear, although it is not apparent in the still photographs. The nonreacting iso-thermal jet (cold jet) in Fig. 4-b also displays the typical shape of large-scale vortical structure up to the blowout. Moreover, the flame formed due to the reaction keeps up the same shape (counter-rotating vortices) as the non-reacting jet by the strong effect of these vortical motions. Therefore, it is inferred that the behavior of the flame base is strongly affected by the large-scale structure of the counter-rotating vortices, which prevail in the iso-thermal jet.

3) Mixing characteristics of the non-reacting iso-thermal jet

In order to investigate the mixing structure of the flame base in the lower blowout limit, we employed the RMS techniques focusing our attention on the counter-rotating vortices that

developed along the jet trajectory because the flow upstream of lifted flame base near blowout behaves basically as a cold jet flow. Figure 5 gives a the planar visualization of the nonreacting iso-thermal jet with cross flow at the three cross-sectional planes (Y-Z plane at X=0) of X = 7, 12, 16d_o with a nozzle diameter of 3.1 mm. For a nozzle diameter of 3.1 mm, the blowout jet velocity of the lower stability limit is 21.04 ms^{-1} when the cross flow velocity is fixed with 3 ms^{-1}. While the iso-thermal jet location shown in Fig.5-b is the same as position of the flame base near blowout in case of flame existence. Namely, X = 12 d_o is the location corresponding to the blowout distance. Figures 5-a and 5-c correspond to the upstream (non-reacting jet region below the flame base) and downstream (flame region) of the flame base, respectively. Comparing Figures 5-b and 5-c with Fig. 5-a, observe the obvious shape of the counter-rotating vortices. From the visualizing pictures, it is ascertained that the mixing structure of non-reacting jet at the position corresponding to the flame base near the blowout is closely related to the mixing structure of large-scale vortices representing the counter-rotating vortices.

3.2 Application of a large-scale structural mixing model

In the preceding section, we identified the mixing structure having large-scale structural vortices at the flame base of the blowout distance for the lower stability limit. Now we introduce the large-scale structural mixing model proposed by Broadwell et at. [13]. Here, we present only a brief concept of this model; additional details can be found in Ref. 13, 14. In their model, the blowout parameter ε was suggested as the necessary condition for flame blowout, where τ_d and τ_c are times required for turbulent mixing and flame ignition, respectively. The blowout parameter ε can be expressed as follows :

$$\varepsilon = \frac{local\ mixing\ time\ (\tau_d)}{characteristic\ chemical\ reaction\ time\ (\tau_c)} = \frac{(d_{b,o} \ / \ u_{b,o})}{(\kappa \ / \ S_b^{\ 2})}$$

where $d_{b,o}$, $u_{b,o}$ are a local diameter and a jet velocity in the location where the blowout occurs, and κ, S_b are a thermal diffusivity and a laminar burning velocity.

In this concept, blowout occurs when hot product gases, which have been expelled to the edge of the jet by earlier large-scale turbulent structures, are reentrained and ignite non-combusting eddies of the jet. If the mixing time of the reentrained gases is too short, the gases cool rapidly and ignition becomes impossible. Therefore, Broadwell et at. thought that the flame blowout was the product of a balance between a chemical time scale (based on a laminar burning velocity) and a physical mixing time scale (based on the known large-scale mixing behavior of turbulent flow field). Basically, a chemically-reacting turbulent mixing layer is envisioned to consist of unmixed fuel and oxidizer streams, homogenized, totally-reacted regions constituting the large vortices. They suggested that the reaction during

homogenization would be extinguished if the local mixing time τ_d becomes sufficiently fast relative to the ignition time τ_c, namely, when the blowout parameter ε defined above falls below a critical value. Consequently, while heating due to entrainment promotes ignition, product dilution facilitates extinction.

By the way, as is well known, mixing behaviors, ranging from nozzle exit to flame base, resemble those in iso-thermal jets. Keffer et al.[1,2] provided experimental equations on the self-similarity of iso-thermal jets in cross flows. Therefore, the local mixing time scale of the cross-flowing jet can be inferred from the above well-known equations, namely, the jet width of Y-direction[2] and the axial mean velocity of ξ-direction[1]. In this case, the deflected jet width ΔY corresponding to the local jet diameter ($d_{b,o}$) can be expressed as

$$\Delta Y = 1.25\ X_{b,o}{}^{0.4}(d_o R')^{0.6},$$

where $X_{b,o}$ is the axial blowout distance and R' is the velocity ratio, defined as $(\rho_j / \rho_w)^{0.5}(U_j / U_w)$.

The axial jet velocity U_c of the ξ direction corresponding to the local jet velocity $u_{b,o}$ is

$$U_c = f(\xi / d_{b,o})(U_j - U_w) + U_w .$$

Also, the jet trajectory equation, which gives the curvilinear distance of the deflected jet, is

$$Z = 2.05 X^{0.28}\ (d_o R')^{0.72}.$$

As a result of applying these equations to this flow field, good agreement between the above equations and the measured results is achieved. From the above expressions, the local mixing time (τ_d) is expressed as

$$\tau_d = d_{b,o} / u_{b,o} = 1.25 \frac{X_{b,o}{}^{0.4}(d_o R')^{0.6}}{f(\xi / d_o)(U_j - U_w) + U_w}.$$

If we know jet exit velocities (U_j), cross air-flow velocities (U_w), blowout distances ($X_{b,o}$), and nozzle diameters (d_o), we can then formulate the blowout parameter ε.

By the way, a precondition to formulating the blowout parameter ε is to find the relevant distance in the flow at which failure of this local stabilization mechanism will lead the flame to blowout. Figure 6 shows the blowout distances in the blowout stability limits of a liftable flame for various nozzle diameters. It is clearly found that although there are 3-dimensional complex structure flames, the blowout distance is always constant for each fixed velocity ratio R (here, $R = U_w / U_j$). The domain of the blowout distances can be classified into three regions according to the velocity ratio R. Regions I, II, and III in Fig.6 correspond to the jet-dominant, transition, cross flow-dominant region, respectively. It decreased stiffly according to the increment of velocity ratio R in Region II (transition region), but decreased slightly in Region III (cross flow-dominant region) where the velocity ratio R is more than 0.1 (for the present work). In particular, it is noted that, in Region III, the distances, projected to the

direction of the cross stream, are always fixed at about $12d_o$ ($X_{b,o} = 12d_o$), even though the blowout distances decrease slightly with the curvilinear coordinate. This is probably the most remarkable observation in the present work.

Figure 7 shows typical still photographs depicting a nozzle with a diameter of 2.2 mm, at which blowout always occurs at $12d_o$ with the straight line in the direction of the cross stream. Although the reason is not clear, one plausible explanation is that the constancy of the blowout distance is closely related to the large-scale structural mixing at the location where the blowout occurs. Therefore, we make it possible to formulate the blowout parameter ε proposed by Broadwell et al.

Figure 8 shows the measured blowout limits for various nozzle diameters investigated, together with the contours of the blowout parameter ε. According to the large-scale mixing model, the blowout parameter ε smaller than a critical value presents the region of the flame blowout, and large values represent the stabilized flame region. Even though there is a quantitative difference in Fig.8, note that in each case, the present blowout formulation predicts the tendency to lower stability limits, which the blowout jet velocity increases with increasing cross flow velocity.

Therefore, there is a necessity for introducing a new variable to explain the blowout mechanism precisely in the cross flow. Because the characteristic chemical time τ_c is a constant value of the physical property in the concept of the large-scale mixing model, it is plausible that such differences appear as a result of the above definition of the local mixing time τ_d in the case of cross flow. When we again formulate the mixing time τ_d considering the velocity ratio R', namely $\frac{(d_{b,o} \cdot R')}{u_{b,o}}$ instead of $\frac{d_{b,o}}{u_{b,o}}$, the comparison in Figure 9 shows that a good quantitative prediction of the measured blowout limits (see Fig. 2) is given by the $\varepsilon' \sim 49$ contour. Fig. 9 gives a comparison of the measured blowout stability limts with the modified contours for the various nozzle diameters investigated in the present work. The contour interval $\Delta\varepsilon'$ is 10, and the blowout is expected at $\varepsilon' \sim 49$ contour, regardless of the nozzle diameters investigated. These results support that the local molecular mixing rate in the flow is the underlying mechanism governing blowout in turbulent nonpremixed jet flames with cross flows. Across the constant average value of contour ($\varepsilon' \sim 49$), the lower values mean the flame always blows out and the upper values mean a stable flame region, which is in agreement with the concept of the large-scale structural mixing model. As we identified in the preceding section, the largest feature in this flow field is the typical large-scale vortical structure, especially at the flame base of the lifted flame near the blowout. The results shown in Fig. 9 confirm that the blowout stability limits of cross-flowing turbulent jet diffusion flame can be formulated in terms of the proposed flame stabilization mechanism based on the large-scale vortical structure, and give clearly accurate predictions for the blowout limits of

such flames. Accordingly, we postulate that the physical mechanism of blowout is due to this large-scale organization of entrainment and mixing observed in the flame base of the lifted flame near the blowout.

Consequently, it is seen that large-scale structures (bound or counter-rotating) play an important role in flame stability in turbulent nonpremixed jet flames with cross flows, especially the blowout.

4 Conclusions

Implication in the earlier study by Kalghatgi[17] gives that the dominant mechanism of blowout is related only to the mixing time of the two flows. That has, therefore, been examined by a modified blowout parameter ε' that is formulated based on Broadwell's large-scale structural mixing model[13]. The main role of the large-scale vortices has also been investigated by experimental observations, and results from the modified blowout parameter ε' are compared with the measured lower blowout limits. From careful observation and comparison, the following conclusions are drawn.

1) The most notable features of the shape of the flame base near the blowout are typical counter-rotating vortices, which are filled with blue flame and always appear on the lower blowout limits, regardless of nozzle diameter. Mixing behaviors in large-scale structures are also ascertained by the RMS technique in a non-reacting iso-thermal jet.

2) The constancy of blowout distance, which is probably the most remarkable observation, has been experimentally observed, and makes it possible to formulate the blowout parameter ε proposed by Broadwell et al. The blowout stability limits have been formulated from the well-known experimental equations[1,2] on the self-similarity of a non-reacting jet in a cross flow. The blowout parameter ε was modified including the velocity ratio R′, and a good correlation between the modified blowout contours and the measured blowout limits confirms the validity of the proposed blowout mechanism. Consequently, the modified blowout parameter ε' reasonably describes the blowout mechanism.

5 Reference

1. KEFFER J F and BAINES W D. The round turbulent jet in a cross-wind. J Fluids Mechanics, 1962, 15, pp 481-496.
2. PRETTE B D and BAINES W D. Profiles of the round turbulent jet in a cross flow. ASCE, HY6, 1967, 92, PP 53-64.

3. MOUSSA Z M, TRISCHKA J and ESKINAZIS. The near field in the mixing of a round jet with a cross-stream. J Fluid Mechanics, 1977, 80, pp 49-80.
4. BROADWELL J E and BREIDENTHAL R E. Structure and mixing of a transverse jet in incompressible flow. J Fluid Mechanics, 1984, 148, pp 405-412.
5. KARAGOZIAN A R. An analytical model for the vorticity associated with a transverse jet. AIAA J, 1986, 24, pp 429-436.
6. GOLLAHALLI S R, BRZUSTOWSKI T A and SULLIVAN H F. Characteristics of a turbulent propane diffusion flame in a cross-wind. Trans CSME, 1975, 3, pp 205-17.
7. GOLLAHALLI S R and MENON R. Combustion characteristics in interacting multiple jets in cross flow. Combust Sci and Tech, 1988, 60, pp 375-389.
8. BIRCH A D and FAIRWEATHER M. An experimental study of a turbulent natural gas jet in a cross flow. Combust Sci and Tech, 1989, 66, pp 217.
9. Y D YOO and H D SHIN. An experimental study of jet-diffusion flames in cross air-flow. J of the Institute of Energy, 1994, 67, pp 121-127.
10. PITTS W M. Assessment of theirs for the behavior and blowout of lifted turbulent jet diffusion flames. 22nd symp (int) on Combustion, 1988, pp 809-816.
11. VANQUICKENBORNE L and VAN TIGGELEN A. The stabilization mechanism of lifted diffusion flames. Combustion and Flames, 1969, 86, pp 59-69.
12. KALGHATGI G T. Blow-out stability of gaseous jet diffusion flames. Part I: In still air. Combust Sci and Tech, 1981, 26, pp 233-239.
13. BROADWELL J E, DAHM W J and MUNGAL M G. Blow-out of turbulent diffusion flames. 20th symp (int) on Combustion, 1984, pp 303-310.
14. DAHM W J A and DIBBLE R D. Co-flowing turbulent jet diffusion flame blowout. 22nd symp (int) on Combustion, 1988, pp 801-808.
15. MIAKE-LYE R C and HAMMER J A. Lifted turbulent jet flames: A stability criterion based on the jet large-scale structure. 22nd symp., 1988, pp 817-824.
16. HUANG R F and CHANG J M. The stability and visualized flame and flow structure of a combusting jet in cross flow. Com. and Flames, 1994, 98, PP 267-278.
17. KALGHATGI G T. Blowout stability of gaseous jet diffusion flames. Part II: Effect of cross wind. Combust Sci and Tech, 1981, 26, pp 241-244.

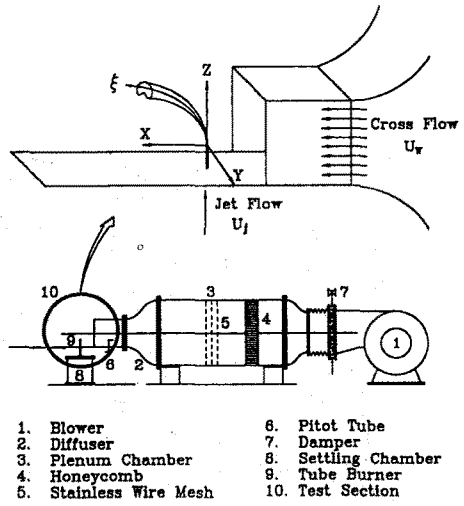

1. Blower
2. Diffuser
3. Plenum Chamber
4. Honeycomb
5. Stainless Wire Mesh
6. Pitot Tube
7. Damper
8. Settling Chamber
9. Tube Burner
10. Test Section

Figure 1. Experimental setup and definition of coordinate system

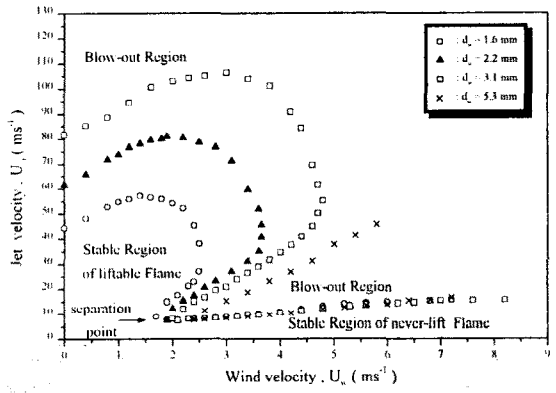

Fig. 2 Blow-out stability limits of combusting propane jet flame with various nozzle diameters in cross flow

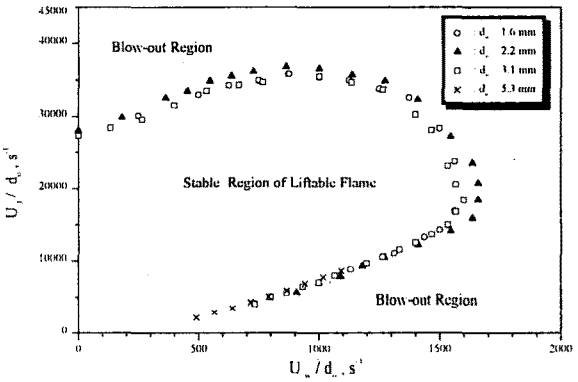

Fig. 3 Common stability curve of combusting propane jet flame with various nozzle diameters in cross flow

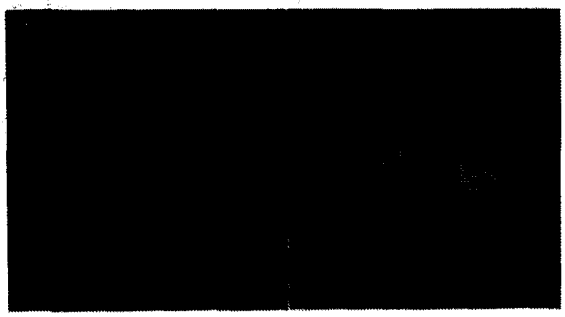

(a) with combustion (b) without combustion

Fig. 4 Photographs showing the flame base and the couter-rotating vortices from an upwind *position for the nozzle diameter of 3.1 mm*

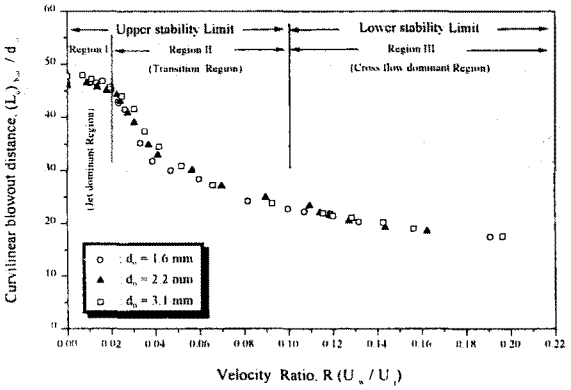

Figure 6. Curvilinear blowout distance according to the velocity ratio R in the blowout stability limits of liftable flame for various nozzle diameters

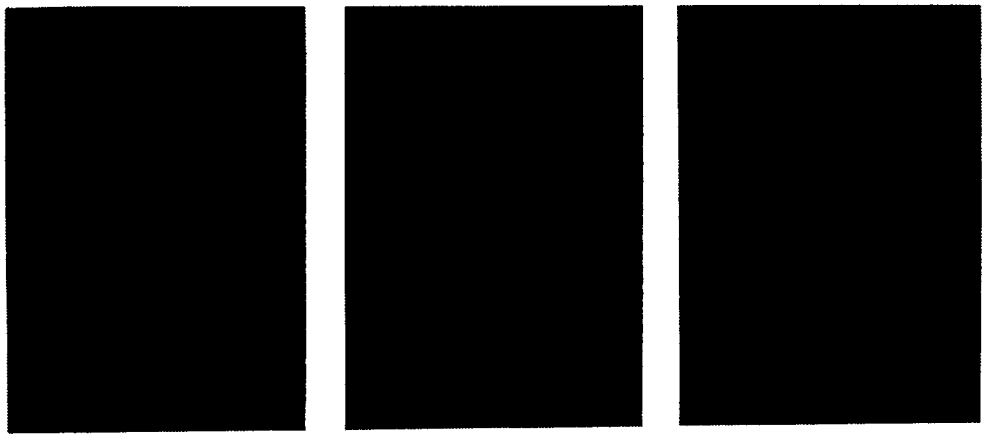

(a) $X = 7\,d_o$ (b) $X = 12\,d_o$ (c) $X = 16\,d_o$

Fig. 5 Cross-sectional views of the non-reacting jet using reactive mie scattering method in the lower limit for the nozzle diameter of 3.1 mm ($U_j = 21.04$ m/s , $U_w = 3.0$ m/s)

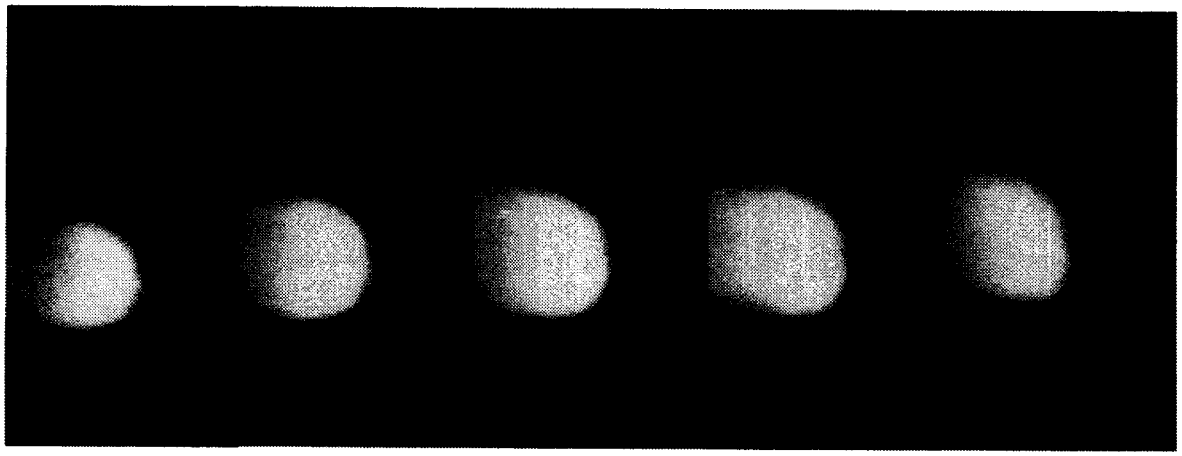

$U_j = 15.3$ m/s	$U_j = 18.8$ m/s	$U_j = 23.0$ m/s	$U_j = 27.0$ m/s	$U_j = 31.0$ m/s
$U_w = 2.2$ m/s	$U_w = 2.5$ m/s	$U_w = 2.8$ m/s	$U_w = 3.1$ m/s	$U_w = 3.4$ m/s

Fig. 7 Typical photographs of a fixed blowout distance with $X_{b.o} = 12\,d_o$ at lower blowout limit of cross-flow dominant region (region III). Data of flow conditions are measured in a $d_o = 2.2$ mm.

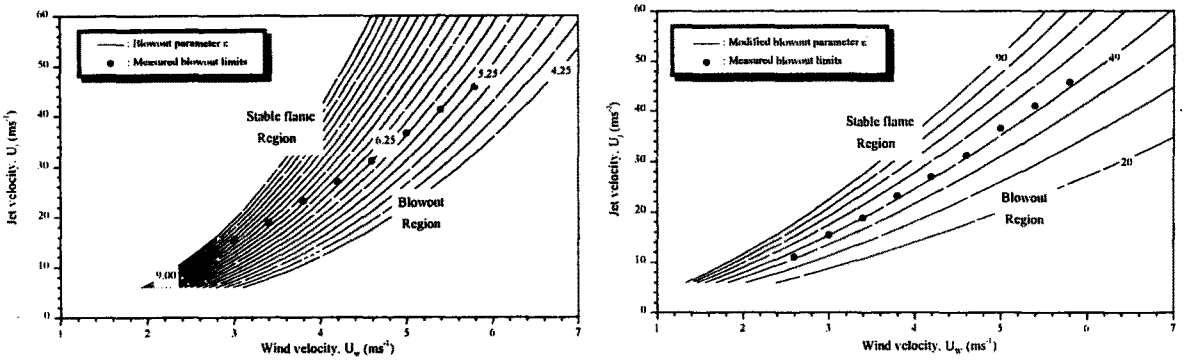

(a) 5.3 mm diameter jet source

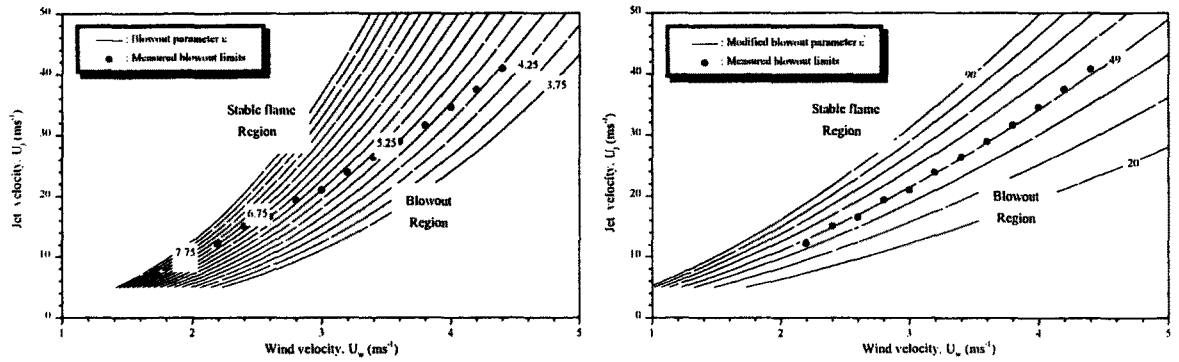

(b) 3.1 mm diameter jet source

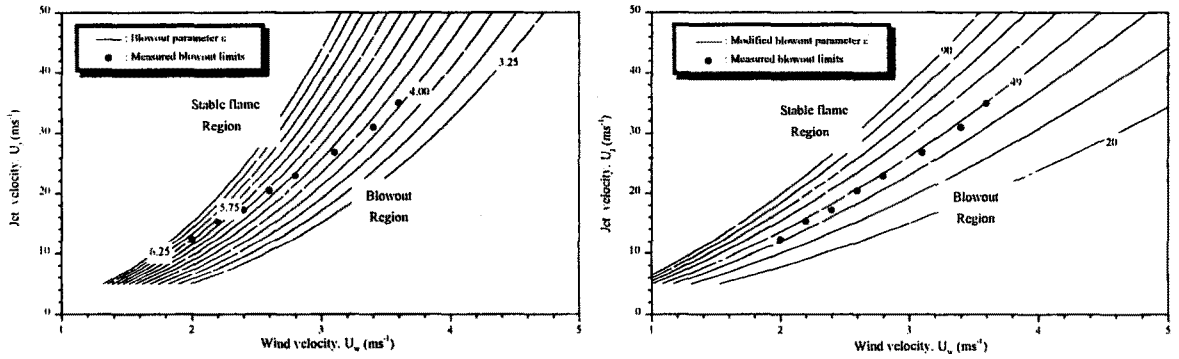

(c) 2.2 mm diameter jet source

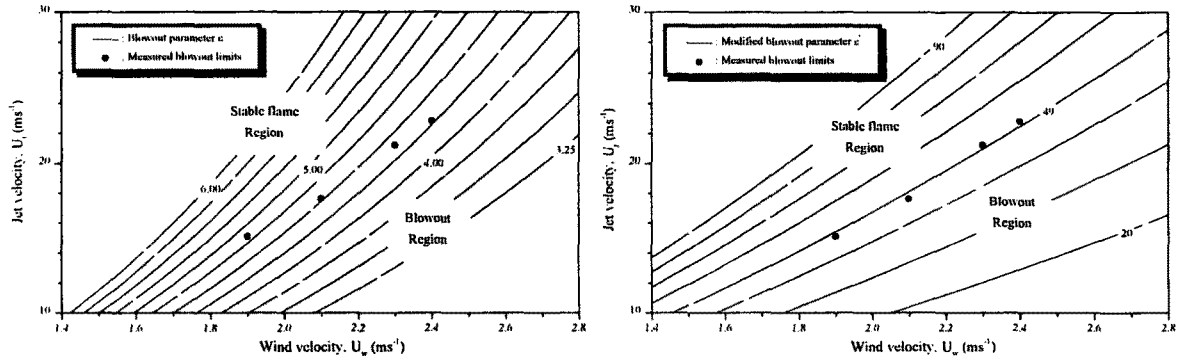

(d) 1.6 mm diameter jet source

Fig. 8 Contours of the blowout parameter ε showing comparisons with the measured lower blowout limits for the various nozzle diameters. Contour interval $\Delta\varepsilon = 0.25$.

Fig. 9 Contours of the modified blowout parameter ε' showing comparisons with the measured lower blowout limits for the various nozzle diameters. Contour interval $\Delta\varepsilon' = 10$. Blowout is expected at $\varepsilon' \sim 49$.